Author Manuscript

Author Manuscript

Author Manuscript

Author Manuscript

HHS Public Access

Author manuscript

Sci Immunol. Author manuscript; available in PMC 2017 June 13.

Published in final edited form as:

Sci Immunol. 2017 February ; 2(8): . doi:10.1126/sciimmunol.aag2152.

Successive annual influenza vaccination induces a recurrent oligoclonotypic memory response in circulating T follicular helper cells

Ramin Sedaghat Herati[1,2,*], **Alexander Muselman**[1,2], **Laura Vella**[2,3], **Bertram Bengsch**[2,4], **Kaela Parkhouse**[5], **Daniel Del Alcazar**[1,2], **Jonathan Kotzin**[2,4], **Susan A. Doyle**[6], **Pablo Tebas**[1], **Scott E. Hensley**[2,4,5], **Laura F. Su**[1,2], **Kenneth E. Schmader**[6], and **E. John Wherry**[2,4,*]

[1]Department of Medicine, University of Pennsylvania Perelman School of Medicine, Philadelphia, PA

[2]Institute for Immunology, University of Pennsylvania Perelman School of Medicine, Philadelphia, PA

[3]Department of Medicine, Children's Hospital of Philadelphia, Philadelphia, PA

[4]Department of Microbiology, University of Pennsylvania Perelman School of Medicine, Philadelphia, PA

[5]Wistar Institute, Philadelphia, PA

[6]Division of Geriatrics, Department of Medicine, Duke University Medical Center and Geriatric Research, Education, and Clinical Center, Durham VA Medical Center, Durham, North Carolina

Abstract

T follicular helper (Tfh) CD4 cells are crucial providers of B cell help during adaptive immune responses. A circulating population of CD4 T cells, termed cTfh, have similarity to lymphoid Tfh, can provide B cell help, and responded to influenza vaccination. However, it is unclear whether human vaccination-induced cTfh respond in an antigen-specific manner and whether they form long-lasting memory. Here, we identified a cTfh population that expressed multiple T cell activation markers and could be readily identified by coexpression of ICOS and CD38. This subset expressed more Bcl-6, c-Maf, and IL-21 than other blood CD4 subsets. Influenza vaccination induced a strong response in the ICOS+CD38+ cTfh at day 7, and this population included hemagglutinin-specific cells by tetramer staining and antigen-stimulated Activation Induced

[*]Correspondence/Reprint Requests: Ramin Sedaghat Herati (ramin.herati@uphs.upenn.edu) or E. John Wherry (wherry@mail.med.upenn.edu).

Author contributions

R.S.H., and E.J.W. conceived the overall design and designed experiments. R.S.H., A.M., L.V., B.B., and J.K. designed and performed Tfh experiments. D.A. and L.S. produced and assisted with tetramer studies. S.D. and K.E.S. recruited and vaccinated study subjects for Cohort 1. P.T. assisted with clinical cohort recruitment for Cohort 2. K.P. and S.E.H. performed hemagglutination inhibition assays. All authors analyzed and interpreted data, discussed the results, and commented on the manuscript. R.S.H. and E.J.W. wrote the manuscript.

Competing financial interests

The authors declare no competing financial interests.

Author Manuscript Author Manuscript Author Manuscript Author Manuscript

Marker (AIM) expression. Moreover, TCRB sequencing identified a clonal response in ICOS +CD38+ cTfh that correlated strongly with the increased circulating ICOS+CD38+ cTfh frequency and the circulating plasmablast response. In subjects who received successive annual vaccinations, a recurrent oligoclonal response was identified in the ICOS+CD38+ cTfh subset at 7 days after every vaccination. These oligoclonal responses in ICOS+CD38+ cTfh after vaccination persisted in the ICOS−CD38− cTfh repertoire in subsequent years, suggesting clonal maintenance in a memory reservoir in the more-stable ICOS−CD38− cTfh subset. These data highlight the antigen-specificity, lineage relationships and memory properties of human cTfh responses to vaccination, providing new avenues for tracking and monitoring cTfh responses during infection and vaccination in humans.

The development of class-switched, affinity-matured antibody production by B cells is dependent on help from T follicular helper (Tfh) cells in the germinal center (1). A circulating subset of CD4 T cells, termed circulating Tfh (cTfh), express CXCR5 and Programmed Death-1 (PD-1) and share phenotypic, functional, and transcriptional properties with lymphoid Tfh (2–4). Vaccine-induced changes in cTfh have been linked to changes in the influenza-specific antibody production. For example, increased expression of inducible costimulator (ICOS; CD278) by cTfh correlated with vaccine-induced antibodies following influenza vaccination (5, 6). Due to the central role of Tfh in antibody development, rational vaccine strategies will benefit from a better understanding of the properties of cTfh during an immune response.

Despite elegant work on the biology of Tfh in animal models and humans, our understanding of how antigen-specific Tfh are induced and maintained in humans is incomplete. Antigen-specific Tfh are generated following an immune stimulus in mice (7), and memory Tfh have been identified (8, 9). In humans, tetanus-specific cTfh have been identified at baseline in healthy adults (3) and antigen-specific Tfh can be detected following challenge with influenza vaccine (6) and HIV vaccine (10). In humans, protective antibody responses following influenza vaccination target hemagglutinin (11). However, although hemagglutinin-specific CD4 T cell responses to vaccination are observed (12), more CD4 T cells respond to the internally conserved influenza proteins than to hemagglutinin (13, 14). This biased specificity may not be true for Tfh, as Tfh may preferentially respond to hemagglutinin rather than nucleoprotein (15), but the dynamics of antigen-specific Tfh responses in humans following vaccination remain poorly understood.

Unfortunately, typical methods to study antigen specificity of CD4 T cells have drawbacks when applied to Tfh. MHC Class II tetramer studies require reagents fitting a cohort of HLA-matched subjects and profile only a fraction of the overall response. Strategies to sort cells based on cytokine production after peptide stimulation have limitations for these analyses, as intrinsic affinity of a TCR for its cognate antigen or incomplete cytokine production by the population of interest only reveal a subpopulation of the cells of interest (16). Proliferation as a marker of antigen-specificity (17, 18) may also lead to a suboptimal picture as Tfh proliferate less than Th1-type CD4 T cells (19). Next-generation methods such as TCRseq (17, 20, 21) permit broad, detailed analysis of the TCR repertoire, but TCRseq has not previously been used to probe Tfh repertoire dynamics.

Author Manuscript Author Manuscript Author Manuscript Author Manuscript

In this study, we identified a subset of cTfh coexpressing ICOS and CD38 that expressed Bcl6, expressed markers of activation such as Ki67 and Helios, and increased in frequency following influenza vaccination. This ICOS+ CD38+ cTfh subset contained cells specific for the $HA_{306–318}$ and $HA_{398–410}$ epitopes. Moreover, ~20–40% of this ICOS+CD38+ cTfh subset induced by influenza vaccination was specific for influenza peptides based on upregulation of activation induced markers following antigen-specific stimulation. Following vaccination, this ICOS+CD38+ subset of cTfh showed repertoire narrowing, indicating antigen-specific expansion of cTfh clones following vaccination. Repeated vaccination of the same subjects recalled highly overlapping clones in successive years indicating robust cTfh memory to influenza vaccination. Analysis of tetramer-specific and activation-induced clonotypes confirmed the presence of influenza-specific clones in the oligoclonal response. Some clones identified in the expanded ICOS+CD38+ cTfh subset on d7 post vaccination were later found in the ICOS−CD38− cTfh population suggesting that ICOS−CD38− cTfh form a pool of memory cTfh that can be repeatedly recalled upon subsequent exposures to antigen. These data provide a tractable way to monitor antigen-induced cTfh responses and identify a pool of memory cTfh that can be repeatedly recalled upon subsequent antigen exposure. Monitoring or specifically targeting these Tfh populations should provide opportunities to further understand and optimize rational vaccine strategies.

Results

Highly activated phenotype of ICOS+CD38+ cTfh at baseline

We first reasoned that recently activated Tfh in the circulation might be identified by the expression of proteins associated with cellular activation. We focused on cTfh, defined as non-naive CD4+CXCR5+PD-1+, that: expressed high levels of the costimulatory marker ICOS that is expressed by lymphoid Tfh (1), contributed to *in vitro* B cell help (3), and were induced in cTfh following influenza vaccination (5, 6). Of circulating cTfh at baseline, ~5% expressed ICOS and also CD38 (hereafter referred to as ICOS+CD38+ cTfh and compared to ICOS−CD38− cTfh). These ICOS+CD38+ cTfh expressed multiple other markers of cellular activation. Directly *ex vivo*, ICOS+CD38+ cTfh had higher expression of CD25, CD27, CD28, CTLA4, PD-1, Helios, and Ki67 and lower expression of CD127 than ICOS −CD38− cTfh (Figure 1A–C). Higher expression of CD3 and CD4 were also observed in ICOS+CD38+ cTfh compared to ICOS−CD38− cTfh, but CXCR5 expression was similar (Figure S1A). This pattern of activation markers was comparable in cryopreserved and freshly isolated PBMC (data not shown). High expression of CD25, CD27, CD39, CTLA4, and Helios was observed even in the absence of Foxp3 (Figure S1B). In sum, ICOS+CD38+ cTfh were a small fraction of all cTfh but expressed many proteins associated with T cell activation.

Activated cTfh express Bcl6 and can produce IL-10, IL-17, and IL-21

Bcl6 has a central role in the Tfh program (1) but protein expression was not detected in total peripheral blood cTfh in prior studies (2, 3, 5). To address whether ICOS+CD38+ cTfh may resemble lymphoid Tfh more than other cTfh, we evaluated expression of Bcl6 protein in the ICOS+CD38+ subset, as well as the expression of other key Th transcription factors and cytokine production. In peripheral blood, Bcl6 protein and mRNA transcript expression

Author Manuscript Author Manuscript Author Manuscript Author Manuscript

was highest in ICOS+CD38+ cTfh compared with ICOS−CD38− cTfh or CXCR5− memory CD4 T cells but was lower than in splenic germinal center Tfh (Figure 2A, Figure S2A–D), suggesting that the ICOS+CD38+ cTfh subset bear closer resemblance to lymphoid Tfh than ICOS−CD38− cTfh. Moreover, expression of Bcl6 was highest in the ICOS+CD38+ cTfh with the highest PD-1 expression (Figure 2B).

Prior studies have suggested Th1-, Th2-, and Th17-polarized subsets exist within the cTfh pool (2), but other studies have found low expression of master transcriptional regulators such as Tbet or RORγT in Tfh (22, 23). To address whether cTfh expressed these regulators, protein expression of these transcription factors was profiled in cTfh. The majority of activated cTfh lacked detectable expression of any of these lineage-associated transcription factors (Figure 2C, Figure S2E). Of these, Tbet was most commonly expressed in ICOS+CD38+ cTfh. T follicular regulatory cells (Tfr) were identified by expression of Foxp3 and CD25 and represented approximately 5% of the ICOS+CD38+ cTfh, consistent with the frequency of circulating Tfr from mouse studies (24). The transcription factor c-Maf has a critical role in Tfh biology (25–27) and displayed high expression in ICOS+CD38+ cTfh, as did total Foxo1. GATA3 is critical for development, maintenance, and function of lymphocytes (28) and was higher in ICOS+CD38+ cTfh compared to ICOS−CD38− cTfh (Figure 2C). Coexpression of Tbet and RORγT or GATA3 was observed in a minority of ICOS+CD38+ but not ICOS−CD38− cTfh (Figure 2D, Figure S2F). Thus, the ICOS+CD38+ cTfh subset expressed Bcl6 and c-Maf protein, but few cells expressed Tbet, RORγT, or Foxp3.

To investigate the cytokine profile of cTfh, we next performed *ex vivo* stimulation and intracellular cytokine staining for cytokines associated with T helper subsets and important for germinal center reactions (1), including IL-17 (29) and IL-10 (30). Upon stimulation with PMA/ionomycin, ICOS+CD38+ cTfh produced a unique combination of IL-10, IL-17, and IL-21 compared to other CD4 subsets (Figure 2E, Figure S2G–I). Similar findings were observed when PBMC were stimulated with SEB (data not shown). Of note, ICOS+CD38+ cTfh were the strongest producers of IL-21 compared to other subsets. Indeed, the frequency of IL-21-producing cells in the ICOS+CD38+ cTfh subset was two-fold higher than the frequency in the ICOS−CD38− cTfh and three-fold higher than CXCR5− memory CD4. Overall, ~1/3 of ICOS+CD38+ cTfh expressed none of the assayed cytokines, ~1/3 expressed TNFα alone, and the remainder co-expressed multiple cytokines, primarily IL-10 and IFNγ (Figure 2F, Figure S2H). Most IL-17^{+} ICOS+CD38+ cTfh also produced IFNγ and TNFα. There was greater polyfunctionality in the ICOS+CD38+ cTfh than ICOS−CD38− cTfh, consistent with their activation state. While the majority of ICOS+CD38+ cTfh were capable of production of TNFα, this subset produced more IL-21, supporting the hypothesis that ICOS+CD38+ cTfh are more similar to lymphoid Tfh than ICOS−CD38− cTfh.

Influenza-specific cells can be identified within ICOS+CD38+ cTfh subset following influenza vaccination

We and others previously observed increased expression of ICOS among cTfh following influenza vaccination (5, 6). We next wanted to investigate whether protein expression of

Author Manuscript Author Manuscript Author Manuscript Author Manuscript

other markers of activation changed after immunization. Subjects in Cohort 1 (Table S1) received inactivated influenza vaccine during the Fall of 2014 (n=28). In an influenza challenge study, a subset of CD4 coexpressing CD38-Ki67 was observed one week after infection (13). In our cohort one week after vaccination we observed increased CD38 expression among nonnaive Ki67+ CD4 T cells (Figure 3A; Figure S3A). Prior to vaccination, cTfh represented ~25% of the Ki67+CD38+ CD4 T cells. Following vaccination, the proportion of cTfh in this Ki67+CD38+ CD4 T cell compartment increased between 4%–60% (Figure 3A–B). By instead gating directly on nonnaive CXCR5+PD-1+ CD4, we observed a vaccine-induced increase of 20%–60% in this subset of ICOS+CD38+ cTfh (Figure 3C, Figure S3B). Expression of PD-1 also increased in the ICOS+CD38+ cTfh following vaccination (Figure S3C–D), but no changes were detected with respect to expression of CD25, CD27, CD28, CD127, CTLA4, Helios, or Ki67 (data not shown). Of the nonnaive Ki67+CD38+ CD4 cells that were CXCR5−, there was no clear phenotypic change following influenza vaccination (data not shown). Thus, influenza vaccination was associated with increased frequency of the ICOS+CD38+ cTfh population.

We next hypothesized that the day 7 ICOS+CD38+ cTfh population would be enriched for influenza-specific cells. Prior studies have identified CD4 T cells specific for nucleoprotein (NP), matrix 1 (M), and hemagglutinin (HA) peptides following vaccination (13, 14, 31). However, these methods typically rely on cytokine production after stimulation. We observed production of TNFα, IFNγ, or IL-2 by only a minority of cTfh following stimulation with overlapping peptide pools for influenza proteins (HA-1, HA-3, NP, and M, data not shown), and IL-21 was produced by only a subset of cTfh following PMA/ionomycin stimulation (Figure 2E). Here, an independent approach using class II tetramers was employed (32). A second cohort of subjects was recruited (n=12, Table S1) and a similar ICOS+CD38+ cTfh response was observed one week after vaccination (data not shown). We examined HLA class II/peptide tetramer+ CD4 T cells at one week following vaccination in two HLA-DRB1*04:01 subjects. CD4 T cells specific for either HA residues 306–318 ($HA_{306–318}$) or HA residues 398–410 ($HA_{398–410}$) (12, 32, 33) were identified in these subjects, including clear HA-specific cTfh (Figure 3D). Of these HA tetramer+ cTfh, 50–91% co-expressed ICOS and CD38. Following influenza vaccination the majority of these tetramer-positive cTfh also expressed CXCR3 (Figure S3E), consistent with prior reports (6). Thus, the identification of influenza HA-specific cells in the cTfh subset one week after inactivated influenza vaccine suggests that antigen-specific cTfh were indeed induced by vaccination and could be found in the ICOS+CD38+ cTfh subset.

Although tetramer staining clearly demonstrated that influenza-specific CD4 T cells are contained in the ICOS+CD38+ cTfh population following vaccination, a tetramer-based approach is likely to underestimate the total influenza vaccine-induced population as few epitopes were interrogated. Expression of activation-induced markers (AIM) has been used to identify antigen-specific CD4 T cells following antigen stimulation (34, 35). This approach has the advantage of not being restricted to a single epitope specificity and offers a broader view of antigen-specific cTfh populations. Thus, to complement the tetramer approach, PBMC pre and post vaccination were stimulated with overlapping influenza peptide pools for NP, M, H1, and H3 for 18 hours. After stimulation of PBMC from day 7 post vaccination, we observed a clear population of antigen-specific ICOS+CD38+ cTfh

Author Manuscript Author Manuscript Author Manuscript Author Manuscript

identified by upregulation of CD69 and CD200 (Figure 3E–F). This population was not present in unstimulated controls (Figure S3F) and was 30- to 150-fold higher at day 7 post vaccination compared to day 0 in the ICOS+CD38+ population or compared to the ICOS −CD38− cTfh subset (Figure 3E–F, Figure S3F). We did not observe an increase in the overall frequency of ICOS+CD38+ cTfh following 18-hour stimulation (data not shown), suggesting that acquisition of ICOS and CD38 either requires a longer period of stimulation, stronger stimulus, or perhaps other signals. Together, these data demonstrate the presence of robust influenza-specific responses within the ICOS+CD38+ cTfh population at day 7 after influenza vaccination.

Increased clonality of ICOS+CD38+ cTfh following influenza vaccination

Compared to other CD4 T cell populations, the ICOS+CD38+ cTfh subset was enriched for influenza-specific cells based on tetramer and response to influenza antigen stimulation *in vitro* (AIM analysis). To examine the clonotypes in the vaccine response more broadly, T cell receptor sequencing (TCRseq) from multiplex PCR amplification of genomic DNA (20) was employed on sorted cTfh populations. In most subjects, clonality of the ICOS+CD38+ cTfh population increased following influenza vaccination (Figure 4A–B, Figure S4A–B). The ICOS−CD38− cTfh had reduced clonality following vaccination but this did not correlate with the increase in clonality in ICOS+CD38+ cTfh (Pearson r=−0.16) (Figure S4A). The day 7 response in ICOS+CD38+ cTfh was typified by the small but clear increase of many clonotypes, rather than dominance of a single expanded clonotype. Another measure of clonal dominance, the Gini Index, correlated strongly with clonality and corroborated these results (Figure S4C–D). Correlations were observed between the change in frequency of the ICOS+CD38+ cTfh population and clonality, both when examining day 7 alone as well as when the fold-change at day 7 vs day 0 was examined (Figure 4C and Figure S4E). We did not detect a clear relationship with the hemagglutination-inhibition antibody titer and ICOS+CD38+ cTfh clonality (Figure S4F–G), perhaps reflecting the fact that hemagglutination-inhibition antibody is only a small fraction of the total antibody induced by vaccination. However, the change in clonality of ICOS+CD38+ cTfh did correlate with the change in frequency of circulating plasmablasts (Figure 4D–E), suggesting a relationship between this cTfh subpopulation and the humoral immune response. These data demonstrate a rapid, oligoclonal ICOS+CD38+ cTfh response to vaccination that strongly correlated with the magnitude of the response. Influenza vaccination resulted in antigen-specific expansion of cTfh populations that could be observed in the PBMC and had a connection to the overall B cell response.

Repeated influenza vaccinations elicit a recurring oligoclonal response

Nearly all humans become seropositive for influenza virus specific antibodies by the end of childhood (36). Thus, we assumed that, prior to entry into the study, all adult subjects had either been immunized against, or been infected with, influenza A virus at least once in the past. However, it was unknown whether a recall response with successive vaccinations would elicit the same oligoclonal response, given the passage of time, the annual reformulation of the influenza vaccine, and the possibility of influenza infection prior to re-vaccination. For six of the subjects in Cohort 2, cryopreserved PBMC were available following influenza vaccination over multiple years. Of these, four had PBMC available for

Author Manuscript Author Manuscript Author Manuscript Author Manuscript

the 2014–2015 and 2015–2016 vaccination years and two had PBMC available for the 2013–2014, 2014–2015 and 2015–2016 vaccination years. Repeated induction of ICOS +CD38+ cTfh was observed at day 7 following each successive vaccination (Figure 5A and Figure S5A).

We first investigated the stability of the cTfh repertoire over time, independent of vaccination. The overlap score (**Materials and Methods**) provides an estimate of similarity in repertoire of a population of T cells across different time points. To assess this, similarity of the TCRB repertoire of each subset was compared to itself one year post vaccination (i.e. just prior to re-vaccination). The ICOS+CD38+ cTfh subset had low overlap score over 1 year in the same individual suggesting high turnover of this subset of cTfh in the absence of vaccination (Figure 5B). In contrast, the ICOS−CD38− cTfh and CXCR5− memory CD4 subsets had more stable TCR repertoires over time. Among these populations, the ICOS −CD38− cTfh subset had more overlap across one year than the CXCR5− memory subset. These observations indicate more dynamic turnover in the clones contained in the ICOS +CD38+ subset compared to the ICOS−CD38− subset of cTfh in the steady state.

We next considered the effect of vaccination on the TCRB repertoire of these CD4 T cell populations. There was essentially no overlap when comparing the ICOS+CD38+ repertoire at Year 1 Day 7 post vaccination to Year 2 Day 0, indicating that, within the limit of detection of these assays, the clones present in the ICOS+CD38+ cTfh subset following influenza vaccination were no longer detectable in this subset a year later (Figure 5C). However, on day 7 post vaccination in Year 2, clones from the Year 1 post vaccination ICOS +CD38+ cTfh subset re-emerged in the ICOS+CD38+ cTfh subset. Neither the ICOS −CD38− cTfh nor CXCR5- memory CD4 subsets showed such a response (Figure 5D and Figure S5B). The timing of the vaccination in the prior years did not have an apparent effect on the recall responses in ICOS+CD38+ cTfh (Figure S5B). The median number of clonotypes in the recurrent oligoclonal response for all subjects was 66 but varied widely from subject to subject and did not appear dependent on number of years of observation (Figure 5E). These data strongly suggested a recurrent oligoclonal response in the ICOS +CD38+ cTfh subset to repeated influenza vaccination in all subjects.

To investigate these clonality relationships in more detail, we focused on the two subjects for whom three years of data were available. There was a robust increase in overlapping clonotypes between Year 1 Day 7 and subsequent Day 7 time points, but we observed only weak overlap with subsequent Day 0 time points in the ICOS+CD38+ cTfh subset (Figure 5F and Figure S5B–C). Moreover, clones shared at every Day 7 time point in ICOS+CD38+ cTfh were absent at every Day 0 time point, whereas clones shared at every Day 7 time point in ICOS−CD38− cTfh or CXCR5− memory were sometimes present at Day 0 time points in these subsets as well (Figure 5G and Figure S5D) suggesting more stability in the clonality of the latter subsets. Rare clones in the ICOS−CD38− cTfh and CXCR5− subsets demonstrated the same pattern as the ICOS+CD38+ cTfh subset and increased in frequency after vaccination, suggesting possible influenza vaccine responses in these subsets. For clones shared at every Day 7 time point in ICOS+CD38+ cTfh, there was no quantitative change in the median frequency at each Day 7 time point, arguing against successive quantitative boosting with each vaccination (Figure S5E). Finally, a cumulative frequency

Author Manuscript Author Manuscript Author Manuscript Author Manuscript

was obtained by adding together all of the frequencies for the Year 1 Day 7 clonotypes in the Year 2 Day 0 time point. The cumulative frequency of the recurrent oligoclonal response clones ranged from 6–15% of the total ICOS+CD38+ cTfh subset (Figure 5H). Together, these data demonstrate considerable clonal dynamics in the ICOS+CD38+ subset of cTfh, suggesting that this subset contains transient clones responding to recent antigenic stimulation. Moreover, these observations support the idea that influenza vaccination induces a repeated recall of conserved clonotypes in the ICOS+CD38+ cTfh following each yearly vaccination.

Influenza-specific clonotypes are contained within the recurring oligoclonal response

The increase in circulating frequency of ICOS+CD38+ cTfh after influenza vaccination was observed consistently in nearly every subject. We hypothesized that clonotypes identified by tetramer or AIM strategies should thus be enriched in the ICOS+CD38+ cTfh subset at one week after vaccination. To test this idea, we sorted $HA_{308–316}$ or $HA_{398–410}$-positive CD4 T cells at 6 months post vaccination. At this time point, none of the tetramer+ CD4 T cells were ICOS+CD38+ (Figure 6A–B, Figure S6A). We then sequenced TCRB changes of these cells and compared the TCRB sequences to those previously obtained from the total ICOS+CD38+ cTfh on day 7 post vaccination. Despite only obtaining only a small number of TCRB sequences (n=10–35) due to the low frequency of tetramer+ CD4 T cells, there was clear overlap of the tetramer-specific clonotypes with the bulk ICOS+CD38+ cTfh subset at the day 7 time point each year for both tetramers for one of the two subjects examined (Figure 6A, Figure S6B). Even when only a single $HA_{398–410}$ clonotype in Subject 999 was identified within the recurring ICOS+CD38+ cTfh oligoclonal response, this finding was highly unlikely by chance alone (p=0.0002 by Fisher's Exact test). The tetramer clonotypes together comprised 0.37–0.70% of the ICOS+CD38+ cTfh population at day 7 after vaccination each year for Subject 999 (Figure 6B). The inability to detect shared clones between tetramer+ CD4 T cells and the ICOS+CD38+ cTfh subset in Subject 108 (Figure S6C) was likely due to the low number of tetramer events that could be captured 6 months after vaccination in this subject, suggesting either involvement of other specificities in the cTfh response, or that capturing only 10–30 TCRB sequences for a single epitope specificity may be at the limit of detection for this type of analysis.

To further explore these questions and test whether the ICOS+CD38+ cTfh population contained influenza-specific cells in a manner that did not depend on HLA-class II tetramers, we next employed the AIM approach described above. As above, PBMC were stimulated with pools of influenza peptides and CD69+CD200+ICOS+CD38+ cTfh were sort purified on day 7 after influenza vaccination. Using this approach we identified 33–216 clonotypes by TCRseq, depending on the subject (Figure S6D). Many TCRB sequences were identified in the influenza-specific AIM approach that were shared with TCR sequences identified in the total ICOS+CD38+ cTfh subset at day 7 post vaccination of each year (Figure 6C, Figure S6E). Again similar to the recurring oligoclonal response, the AIM clonotypes showed similar pattern of increased frequency in the ICOS+CD38+ cTfh subset at each day 7 time point in three of the six subjects (Figure 6D). The overlap between the recurrent oligoclonal response and the AIM clonotypes was statistically significant in four of six subjects (Figure 6E, Figure S6F). Of note, AIM clones and recurring oligoclonal

Author Manuscript Author Manuscript Author Manuscript Author Manuscript

response clones were not prominently found in other subsets, suggesting strong enrichment for influenza specific clones in the cTfh compartment (Figure S6G–H), though because the non-cTfh compartments are substantially larger, undersampling cannot be excluded. Nevertheless, these data confirm the presence of influenza-specific clonotypes within the ICOS+CD38+ cTfh subset one week after each influenza vaccination, as well as within the yearly recurring oligoclonal response.

ICOS−CD38− cTfh may serve as a long-term reservoir of cTfh memory

The TCRB sequence has been used as a "fingerprint" to track clones through different compartments in other studies (37–39), although a particular clone could sometimes be found in multiple distinct CD4 subsets (40). Here, to track clones across subsets over time, clones present for each subset at Year 1 Day 7 were compared against all the other subsets at Year 2 (Figure 7A–C and Figure S7A). A cumulative frequency was obtained by adding together all of the frequencies for the Year 1 Day 7 clonotypes in the Year 2 Day 0 time point. As expected, clones that were originally present in the CXCR5− memory or ICOS −CD38− cTfh subsets in Year 1 Day 7 could be found in the CXCR5− memory (Figure 7A) or ICOS−CD38− cTfh (Figure 7B) subsets at Year 2 Day 0. Clones present in the ICOS −CD38− cTfh in Year 1 Day 7 were most frequently found in the ICOS−CD38− cTfh subset at Year 2 Day 0 (Figure 7B), consistent with the higher overlap scores for ICOS−CD38− cTfh at one year in Figure 5B.

Given the relative stability and greater circulating frequency of the ICOS−CD38− cTfh subset compared to ICOS+CD38+ cTfh, we hypothesized that ICOS−CD38− cTfh represented a long-term "reservoir" for cTfh from which specific clones may be recalled into the ICOS+CD38+ cTfh pool. To test this idea, we asked if clones present at Year 1 Day 7 in the ICOS+CD38+ cTfh could be found in other subsets at Year 2. Indeed, clones present at Year 1 Day 7 in ICOS+CD38+ cTfh were most frequently found in the ICOS−CD38− cTfh subset at Year 2 Day 0 (Figure 7C). Similarly, ICOS+CD38+ cTfh clones present at Year 2 Day 7 were most frequently found in ICOS−CD38− cTfh at Year 3 Day 0 (Figure 7D, Figure S7B). As noted earlier, influenza vaccination induced an increase in the frequencies of the Year 1 Day 7-matched clonotypes in the ICOS+CD38+ cTfh (Figure S7A), but this effect was not seen in CXCR5− memory or ICOS−CD38− cTfh. Some clones from Year 1 Day 7 ICOS−CD38− cTfh were present in Year 2 Day 0 ICOS+CD38+ cTfh, suggesting some low-level conversion of ICOS−CD38− cTfh to ICOS+CD38+ cTfh.

Together, these data indicate a strong clonal connection between ICOS+CD38+ and ICOS −CD38− cTfh. Clones expanded following influenza vaccination may, therefore, preferentially convert into the ICOS−CD38− cTfh subset. These results support a model where cTfh cycle back and forth between activated and inactive states following repeated antigen exposure, with the ICOS−CD38− cTfh subset representing the reservoir for memory cTfh.

Discussion

Induction of a strong antibody response is a major correlate of protection in nearly all licensed vaccines. Despite the importance for vaccines, our understanding of the Tfh

Author Manuscript Author Manuscript Author Manuscript Author Manuscript

response underlying vaccine-induced antibody responses remains incomplete. In this study, we found that cTfh co-expressing ICOS and CD38 increased in frequency and clonality following influenza vaccination. This subset of cTfh expressed markers of activation and contained influenza virus specific tetramer+ cells at day 7 post vaccination. These data not only identify a proxy for antigen-specific cTfh allowing monitoring of human vaccine-induced responses, but also provide insights into the dynamics of cTfh memory and recall responses.

Although cTfh are thought to be derived from lymphoid tissue, differences have been reported between lymphoid Tfh and cTfh in protein expression including lack of transcription factor Bcl6 expression, leading to uncertainty regarding the ontogeny of this cTfh population (2, 3, 41–43). We observed the highest expression of Bcl6 and greatest production of IL-21 in the ICOS+CD38+ cTfh compared to other cTfh in peripheral blood suggesting a relationship to GC events in lymphoid tissues. It is possible that, given the rapid kinetics of appearance of ICOS+ cTfh following vaccination (6) and the highly activated phenotype of ICOS+CD38+ cTfh we found here, ICOS+CD38+ cTfh are related to memory follicular mantle Tfh-like cells (42), rather than originating from cells that have participated directly in germinal center interactions. Understanding the ontogeny of cTfh and their relationships to other T helper subsets will clarify when and how cTfh can serve as a biomarker of a vaccine response. Nevertheless, in the absence of ready access to human lymphoid tissues in a routine setting, the circulatory ICOS+CD38+ cTfh population may act as a proxy of events occurring in the lymphoid tissue.

Although memory Tfh have been identified in mice (8, 9), the ability to broadly identify memory Tfh in humans has been limited. Here, use of T cell receptor β chain sequencing allowed identification of the memory Tfh response to influenza vaccination, based on the repeated induction of an oligoclonal response containing influenza specific cells in the ICOS +CD38+ cTfh. The clonal composition of this response repeated with each vaccination, despite the annual vaccine reformulation and possible intercurrent influenza infection. Recall of the same clonotypes could reflect the greater immunodominance of relatively conserved internal influenza proteins in CD4 responses (13, 14) or original antigenic sin (44, 45). Moreover, the stability of the recall response repertoire suggests longevity in the influenza-specific CD4 T cell repertoire. It will be interesting to compare the dynamics, quality and repertoire diversity of this ICOS+CD38+ subset of antigen-induced cTfh for different vaccination approaches.

Initial evaluation identified many phenotypic differences between ICOS+CD38+ cTfh and ICOS−CD38− cTfh. It was unclear if these subsets were directly related and whether the repertoire dynamics differed between these subsets. We observed notable stability of the repertoire of ICOS−CD38− cTfh over one year, in contrast to the dynamic changes in the ICOS+CD38+ cTfh. Moreover, the clonotypes from ICOS+CD38+ cTfh and ICOS−CD38− cTfh were observed most frequently in the ICOS−CD38− cTfh subset at Year 2 Day 0. Thus, the ICOS−CD38− cTfh may function as a long-term reservoir from which clones can be selectively re-activated, leading to re-expression of ICOS and CD38. Curiously, some Year 1 Day 7 ICOS+CD38+ cTfh clones were still present in the Year 2 Day 0 ICOS+CD38+ cTfh subset at detectable frequencies. Persistence of clones within the ICOS+CD38+ cTfh subset

Author Manuscript Author Manuscript Author Manuscript Author Manuscript

over many months could reflect ongoing antigenic availability such as from commensal bacteria, viruses, or other environmental antigens. Indeed, the ICOS+CD38+ cTfh subset may provide a novel way to interrogate ongoing immune responses in the steady state with potential application to persisting infections, autoimmunity, and allergy. Overall, these data provide a foundation for tracking cTfh memory and a framework for future studies that should help delineate the relationship of circulating Tfh populations to Tfh in lymphoid tissues.

It is perhaps remarkable that recurrent oligoclonal responses were detectable in the ICOS +CD38+ subset of cTfh, particularly in the setting of an unadjuvanted seasonal influenza vaccine. For example, assuming the circulating frequencies of CD4 T cells is similar across the 5L of human blood volume, there are ~3 million ICOS+CD38+ cTfh total in circulation. In these studies, we sampled from 40–100 mL of blood (or 0.8–2.0% of the total) and only recovered productive TCRB sequences from 10–20% of the cells analyzed (i.e. sampling only 0.08–0.4% of total ICOS+CD38+ cTfh). The likelihood of identifying the same random 50–70 clones at two time points with this sampling approach the among 3 million ICOS +CD38+ cTfh cells is extraordinarily low. Although we are unable to sample and interrogate rare clonotypes by these approaches, these data provide strong evidence for the repeated recruitment of common clonotypes into the antigen-specific cTfh response induce by influenza vaccination. Moreover, based on the AIM analysis we can account for up to 20% of the vaccine-induced ICOS+CD38+ cTfh as antigen-specific (e.g. 11% of ICOS+CD38+ induce CD200 and CD69 (Figure 3E) and ~1/2 of the ICOS+CD38+ cTfh population is induced by vaccination (Figure 3C)). These data are consistent with the clonotypic analysis that identifies up to ~10–20% of the ICOS+CD38+ cTfh (maybe 20–40% if one considers only the increase in the ICOS+CD38+ cTfh population after vaccination) as using TCRB sequences repeatedly recalled by influenza vaccination. Perhaps the remainder of this vaccine induced ICOS+CD38+ cTfh population is non-specific bystander cTfh activation. Alternatively, these cells could represent heterogeneous rare clonotypes and/or specificities not efficiently assayed in the AIM approach. Future studies should be able to address these questions with deeper TCRB analysis and analysis of additional specificities. Nevertheless, these distinct approaches yield data that are not only internally consistent and demonstrate a robust influenza virus-specific cTfh response, but also provide approaches to allow future interrogation of antigen-induced cTfh responses and Tfh memory in humans. The relationship of these cTfh to lymphoid Tfh in terms of function, clonality and dynamics remains to be evaluated. However, one interesting possibility is that the cTfh memory populations identified here using repeated yearly vaccination may be a source of systemic memory allowing new germinal center reactions to be seeded in any lymphoid tissue depending on where the antigen is encountered.

Future rational vaccine strategies may require eliciting precise T cell responses in order to provide help for the desired types and specificities of the antibody response. Identification of the specific TCR repertoire expanded by immunization reveals a broader picture of the cTfh response than typically accessible by HLA class II tetramers or cytokine production following antigen-stimulation. The identification of cTfh memory and the dynamics of this population upon vaccination provides a framework for not only dissecting how these cells are related to lymphoid tissue responses but also provides key insights for evaluating and

Author Manuscript Author Manuscript Author Manuscript Author Manuscript

comparing future vaccination regimens for their ability to induce the designed magnitude and quality of cTfh memory.

Materials and Methods

Human subjects

Subjects were eligible if they were community-dwelling and had not received influenza vaccine in the prior 6 months; they were excluded if they had contraindications to influenza vaccine, active substance abuse, HIV/AIDS, clinically active malignancy, immunomodulatory medication need (i.e. chemotherapy, corticosteroids), or active illness (i.e. active respiratory tract infections). Seasonal inactivated influenza vaccine (Fluvarix, GlaxoSmithKline) was administered and peripheral venous blood was drawn on days 0, 7, and 28 after vaccination. For Cohort 1, study subjects were recruited and consented in the Fall of 2014 at the Clinical Research Unit at Duke University Medical Center (Durham, NC, USA), in accordance with the Institutional Review Boards of both Duke University and the University of Pennsylvania (Philadelphia, PA, USA). Blood was collected into heparinized tubes and shipped overnight to Philadelphia, PA. For Cohort 2, study subjects were recruited and consented in between 2013 and 2015 at the University of Pennsylvania. Samples from 2013–2014 were cryopreserved whereas 2015 samples were used immediately after collection. Human spleen samples from relatively healthy adults were obtained as de-identified excess medical tissue via the Cooperative Human Tissues Network (CHTN), typically after trauma or incidental splenectomy. Splenocytes were obtained by mechanical dissociation and cryopreserved until needed. All human subjects research was performed in accordance with the relevant Institutional Review Boards.

Flow cytometry

Fresh PBMC and plasma were isolated using Ficoll-Paque PLUS (GE Healthcare) or SepMate isolation (Stem Cell Technologies) and stained for surface and intracellular markers. Permeabilization was performed using the Foxp3 Fixation/Permeabilization Concentrate and Diluent kit (eBioscience). Antibodies and clones are described in Table S2. Cells were resuspended in 1% para-formaldehyde until acquisition on a BD Biosciences LSR II cytometer and analyzed using FlowJo (Tree Star) and ViSNE (Cytobank). Fluorescence-minus-one controls were performed in pilot studies. The Bcl6 protein expression analysis was performed on both a BD LSR II (18-color instrument) and also repeated using a BD Symphony A5 (28-color) cytometer. The advantage of the latter experiment was that the Bcl6 antibody was the only reagent used on the violet laser greatly reducing fluorescence spillover from other fluorochromes and substantially improving the signal-to-noise ratio for detection of low protein amounts.

HLA Class II tetramers

HLA Class II tetramers were prepared as previously described (32). Staining by tetramers against hemagglutinin residues 306–318 (PKYVKQNTLKLAT) or hemagglutinin residues 398–410 (SVIEKMNTQFTAV) in two HLA-DRB1*04:01 subjects was performed for 1 hour at room temperature, followed by magnetic bead enrichment at 4°C and fixation. Fixed samples were acquired on a BD Biosciences LSR II cytometer. For sorting experiments,

Author Manuscript Author Manuscript Author Manuscript Author Manuscript

tetramer staining was performed in a similar fashion but samples were maintained unfixed at 4°C until they could be sorted on a BD FACS Aria cell sorter.

Activation-induced marker stimulations

PBMC were thawed and rested overnight at 37°C in RPMI with 10% fetal calf serum and 1% L-glutamine. Overlapping peptide pools for hemagglutinin 1 (A/California/7/2009, catalog #NR-19244), hemagglutinin 3 (A/Perth/16/2009, catalog #NR-19266), nucleoprotein (A/California/7/2009, catalog #NR-18976), and matrix 1 (A/California/7/2009, catalog #NR-18977) were obtained from BEI Bioresources and resuspended in DMSO. Stimulation was performed in flat-bottom plates with 0.5 μg/mL of each peptide pool for 18 hours, followed by surface staining for 20 minutes at room temperature. Acquisition and sorting were performed on a BD FACS Aria cell sorter.

Hemagglutination-inhibition assays

Sera were treated with receptor destroying enzyme and then heated for 30 minutes at 55°C. Sera were serially diluted in 96-well round bottom plates. Four agglutinating doses of A/California/7/2009 or A/Switzerland/9715293/2013 were added to the sera in a total volume of 100 μL. Turkey red blood cells were added (12.5 μL of a 2% (vol/vol) solution)), and agglutination was read out 60 minutes later. Titers are expressed as the inverse sera dilution that inhibited viral agglutination.

RT-qPCR

PBMC and splenocytes were thawed and sorted for subsets on a BD FACS Aria cell sorter followed by RNA extraction by Qiagen Micro Plus kit. Reverse transcription using the High-Capacity Reverse Transcription kit was performed as per manufacturer instructions (Applied Biosystems). Real-time PCR was performed using pre-designed primers and hydrolysis probes for *B2M* (Hs.PT.58v.18759587, IDT) and *BCL6* (Hs.PT.56a.19673829.g, IDT) using the PrimeTime Gene Expression Master Mix (IDT) on a ViiA7 Real-Time PCR system (Applied Biosystems).

T cell receptor sequencing

PBMC were sorted on a BD FACS Aria followed by DNA extraction by Qiagen QIAamp DNA Micro kit. Amplification, library preparation, sequencing, and preliminary bioinformatics analysis was performed by Adaptive Biotechnologies (Seattle, WA). TCRB was sequenced at Survey level resolution.

TCR sequencing analysis

Calculations were performed in R for Shannon's entropy and normalized Shannon's Entropy (46, 47). Gini index was calculated using the R package "ineq" (48). Clonality was calculated as 1 - normalized Shannon's Entropy. The overlap score was calculated as the sum of the counts for all shared sequences observed both in sample A and sample B, divided by the total number of counts for all sequences in samples A and B (shared and unshared) in the two samples. Some figures were generated with packages "ggplot2" and "gplots" (49,

Author Manuscript Author Manuscript Author Manuscript Author Manuscript

50). All R code used for these analyses are available at https://github.com/Sedmic/cTfh_TCRB_2015-2016FluSpec.

Cytokine production

PBMC were stimulated for five hours in the presence of PMA/ionomycin or left unstimulated as a control. Monensin was added for the final four hours of stimulation. Staining was performed at 37°C in the stimulation medium followed by fixation with 1% para-formaldehyde for 5 minutes at room temperature. Cells were then permeabilized with the Foxp3 Fixation/Permeabilization Concentrate and Diluent kit and intracellular staining was performed for one hour at room temperature with antibodies against IL-2, IL-10, IL-13, IL-17, IL-21, TNFα, and IFNγ. Pestle and SPICE (51) were used to analyze polyfunctionality.

Statistics

Statistical analyses were performed with Prism 5 (GraphPad) or with R. Data was compared using Student's *t* test, paired *t* test, or one-way Analysis of Variance (ANOVA) with Tukey post-hoc analysis, as indicated. Correlation analyses were performed as the Pearson correlation. Fisher's Exact test was used to compare overlap in TCR sequences, based on 10^7 theoretical TCRB sequences.

Supplementary Material

Refer to Web version on PubMed Central for supplementary material.

Acknowledgments

R.S.H. was supported by the NIH grants AI114852 and AG047773. K.E.S. was supported in part by the NIH/National Institute on Aging Claude D. Pepper Older Americans Independence Centers (Grant AG028716). This work was supported in part by a grant from the Penn Center for AIDS Research (P30 AI045008). This work was also funded by National Institutes of Health (NIH) grants AI113047 and AI108686 (to S.E.H.), AI112521, AI117950, AI2010085 (to E.J.W.), as well as the U.S. Broad Agency Announcements Grant HHSN272201100018C (to K.E.S. and E.J.W.).

References

1. Crotty S. Follicular helper CD4 T cells (TFH). Annu Rev Immunol. 2011; 29:621–63. [PubMed: 21314428]
2. Morita R, Schmitt N, Bentebibel S, Ranganathan R, Bourdery L, Zurawski G, Foucat E, Dullaers M, Oh S, Sabzghabaei N, Lavecchio EM, Punaro M, Pascual V, Banchereau J, Ueno H. Human blood CXCR5(+)CD4(+) T cells are counterparts of T follicular cells and contain specific subsets that differentially support antibody secretion. Immunity. 2011; 34:108–21. [PubMed: 21215658]
3. Locci M, Havenar-Daughton C, Landais E, Wu J, Kroenke MA, Arlehamn CL, Su LF, Cubas R, Davis MM, Sette A, Elias K, Protocol I, Investigators CP. Poignard P, Crotty S, Haddad EK. Tfh cells are highly functional and correlate with broadly neutralizing HIV antibody responses. Immunity. 2013; 39:1–12. [PubMed: 23890059]
4. Obeng-Adjei N, Portugal S, Tran TM, Yazew TB, Skinner J, Li S, Jain A, Felgner PL, Doumbo OK, Kayentao K, Ongoiba A, Traore B, Crompton PD. Circulating Th1-Cell-type Tfh Cells that Exhibit Impaired B Cell Help Are Preferentially Activated during Acute Malaria in Children. Cell Rep. 2015; 13:425–39. [PubMed: 26440897]
5. Herati RS, Reuter MA, Dolfi DV, Mansfield KD, Aung H, Badwan OZ, Kurupati RK, Kannan S, Ertl H, Schmader KE, Betts MR, Canaday DH, Wherry EJ. Circulating CXCR5+PD-1+ response

Author Manuscript Author Manuscript Author Manuscript Author Manuscript

predicts influenza vaccine antibody responses in young adults but not elderly adults. J Immunol. 2014; 193:3528–37. [PubMed: 25172499]

6. Bentebibel S, Lopez S, Obermoser G, Schmitt N, Mueller C, Harrod C, Flano E, Mejias A, Albrecht RA, Blankenship D, Xu H, Pascual V, Banchereau J, Garcia-Sastre A, Palucka AK, Ramilo O, Ueno H. Induction of ICOS+CXCR3+CXCR5+ TH cells correlates with antibody responses to influenza vaccination. Sci Transl Med. 2013; 5:176ra32.
7. Fazilleau N, Eisenbraun MD, Malherbe L, Ebright JN, Pogue-Caley RR, McHeyzer-Williams LJ, McHeyzer-Williams MG. Lymphoid reservoirs of antigen-specific memory T helper cells. Nat Immunol. 2007; 8:753–61. [PubMed: 17529982]
8. Lüthje K, Kallies A, Shimohakamada Y, Belz GT, Light A, Tarlinton DM, Nutt SL. The development and fate of follicular helper T cells defined by an IL-21 reporter mouse. Nat Immunol. 2012; 13:491–8. [PubMed: 22466669]
9. Liu X, Yan X, Zhong B, Nurieva RI, Wang A, Wang X, Martin-Orozco N, Wang Y, Chang SH, Esplugues E, Flavell Ra, Tian Q, Dong C. Bcl6 expression specifies the T follicular helper cell program in vivo. J Exp Med. 2012; 209:1841–52. S1–24. [PubMed: 22987803]
10. Schultz BT, Teigler JE, Pissani F, Oster AF, Kranias G, Alter G, Marovich M, Eller MA, Dittmer U, Robb ML, Kim JH, Michael NL, Bolton D, Streeck H. Circulating HIV-Specific Interleukin-21(+)CD4(+) T Cells Represent Peripheral Tfh Cells with Antigen-Dependent Helper Functions. Immunity. 2016; 44:167–78. [PubMed: 26795249]
11. Kreijtz JHCM, Fouchier R a M, Rimmelzwaan GF. Immune responses to influenza virus infection. Virus Res. 2011; 162:19–30. [PubMed: 21963677]
12. Danke, Na, Kwok, WW. HLA Class II-Restricted CD4+ T Cell Responses Directed Against Influenza Viral Antigens Postinfluenza Vaccination. J Immunol. 2003; 171:3163–3169. [PubMed: 12960344]
13. Wilkinson TM, Li CKF, Chui CSC, Huang AKY, Perkins M, Liebner JC, Lambkin-Williams R, Gilbert A, Oxford J, Nicholas B, Staples KJ, Dong T, Douek DC, McMichael AJ, Xu XN. Preexisting influenza-specific CD4+ T cells correlate with disease protection against influenza challenge in humans. Nat Med. 2012; 18:274–80. [PubMed: 22286307]
14. Chen L, Zanker D, Xiao K, Wu C, Zou Q, Chen W. Immunodominant CD4+ T-cell responses to influenza A virus in healthy individuals focus on matrix 1 and nucleoprotein. J Virol. 2014; 88:11760–73. [PubMed: 25078703]
15. Leddon SA, Richards KA, Treanor JJ, Sant AJ. Abundance and specificity of influenza reactive circulating memory follicular helper and non-follicular helper CD4 T cells in healthy adults. Immunol. 2015:157–162.
16. Tubo NJ, Pagán AJ, Taylor JJ, Nelson RW, Linehan JL, Ertelt JM, Huseby ES, Way SS, Jenkins MK. Single naive CD4+ T cells from a diverse repertoire produce different effector cell types during infection. Cell. 2013; 153:785–96. [PubMed: 23663778]
17. Qi Q, Cavanagh MM, Le Saux S, Namkoong H, Kim C, Turgano E, Liu Y, Wang C, Mackey S, Swan GE, Dekker CL, Olshen RA, Boyd SD, Weyand CM, Tian L, Goronzy JJ, Le Saux S, Namkoong H, Kim C, Turgano E, Liu Y, Wang C, Mackey S, Swan GE, Dekker CL, Olshen RA, Boyd SD, Weyand CM, Tian L, Goronzy JJ. Diversification of the antigen-specific T cell receptor repertoire after varicella zoster vaccination. Sci Transl Med. 2016; 8:332ra46.
18. Soares A, Govender L, Hughes J, Mavakla W, Kock M de, Barnard C, Pienaar B, van Rensburg E Janse, Jacobs G, Khomba G, Stone L, Abel B, Scriba TJ, Hanekom Wa. Novel application of Ki67 to quantify antigen-specific in vitro lymphoproliferation. J Immunol Methods. 2010; 362:43–50. [PubMed: 20800066]
19. Ray JP, Staron MM, Shyer Ja, Ho P, Marshall HD, Gray SM, Laidlaw BJ, Araki K, Ahmed R, Kaech SM, Craft J. The Interleukin-2-mTORc1 Kinase Axis Defines the Signaling, Differentiation, and Metabolism of T Helper 1 and Follicular B Helper T Cells. Immunity. 2015; 43:690–702. [PubMed: 26410627]
20. Robins HS, Srivastava SK, Campregher PV, Turtle CJ, Andriesen J, Riddell SR, Carlson CS, Warren EH. Overlap and effective size of the human CD8+ T cell receptor repertoire. Sci Transl Med. 2010; 2:47ra64.

Author Manuscript Author Manuscript Author Manuscript Author Manuscript

21. Kirsch I, Vignali M, Robins H. T-cell receptor profiling in cancer. Mol Oncol. 2015; 9:2063–70. [PubMed: 26404496]
22. Schmitt N, Liu Y, Bentebibel SE, Munagala I, Bourdery L, Venuprasad K, Banchereau J, Ueno H. The cytokine TGF-β co-opts signaling via STAT3-STAT4 to promote the differentiation of human TFH cells. Nat Immunol. 2014; 15:856–65. [PubMed: 25064073]
23. Nurieva RI, Chung Y, Hwang D, Yang XO, Kang HS, Ma L, Wang Y, Watowich SS, Jetten AM, Tian Q, Dong C. Generation of T follicular helper cells is mediated by interleukin-21 but independent of T helper 1, 2, or 17 cell lineages. Immunity. 2008; 29:138–49. [PubMed: 18599325]
24. Sage PT, Alvarez D, Godec J, Von Andrian UH, Sharpe AH, von Andrian UH, Sharpe AH. Circulating T follicular regulatory and helper cells have memory-like properties. J Clin Invest. 2014; 124:5191–5204. [PubMed: 25347469]
25. Kroenke, Ma, Eto, D., Locci, M., Cho, M., Davidson, T., Haddad, EK., Crotty, S. Bcl6 and Maf cooperate to instruct human follicular helper CD4 T cell differentiation. J Immunol. 2012; 188:3734–44. [PubMed: 22427637]
26. Liu X, Nurieva RI, Dong C. Transcriptional regulation of follicular T-helper (Tfh) cells. Immunol Rev. 2013; 252:139–45. [PubMed: 23405901]
27. Weber JP, Fuhrmann F, Feist RK, Lahmann A, Al Baz MS, Gentz L-J, Vu Van D, Mages HW, Haftmann C, Riedel R, Grun JR, Schuh W, Kroczek RA, Radbruch A, Mashreghi M-F, Hutloff A. ICOS maintains the T follicular helper cell phenotype by down-regulating Kruppel-like factor 2. J Exp Med. 2015; 212:217–233. [PubMed: 25646266]
28. Wan YY. GATA3: a master of many trades in immune regulation. Trends Immunol. 2014; 35:233–42. [PubMed: 24786134]
29. Hsu HC, Yang P, Wang J, Wu Q, Myers R, Chen J, Yi J, Guentert T, Tousson A, Stanus AL, Le TL, Lorenz RG, Xu H, Kolls JK, Carter RH, Chaplin DD, Williams RW, Mountz JD. Interleukin 17-producing T helper cells and interleukin 17 orchestrate autoreactive germinal center development in autoimmune BXD2 mice. Nat Immunol. 2008; 9:166–75. [PubMed: 18157131]
30. Kim CH, Rott LS, Clark-Lewis I, Campbell DJ, Wu L, Butcher EC. Subspecialization of CXCR5+ T cells: B helper activity is focused in a germinal center-localized subset of CXCR5+ T cells. J Exp Med. 2001; 193:1373–81. [PubMed: 11413192]
31. Dolfi DV, Mansfield KD, Kurupati RK, Kannan S, Doyle Sa, Ertl HCJ, Schmader KE, Wherry EJ. Vaccine-induced boosting of influenza virus-specific CD4 T cells in younger and aged humans. PLoS One. 2013; 8:e77164. [PubMed: 24155927]
32. Su LF, Kidd BA, Han A, Kotzin JJ, Davis MM. Virus-specific CD4(+) memory-phenotype T cells are abundant in unexposed adults. Immunity. 2013; 38:373–83. [PubMed: 23395677]
33. Yang J, James E, Gates TJ, DeLong JH, LaFond RE, Malhotra U, Kwok WW. CD4+ T cells recognize unique and conserved 2009 H1N1 influenza hemagglutinin epitopes after natural infection and vaccination. Int Immunol. 2013; 25:447–457. [PubMed: 23524391]
34. Dan JM, Lindestam Arlehamn CS, Weiskopf D, da Silva Antunes R, Havenar-Daughton C, Reiss SM, Brigger M, Bothwell M, Sette A, Crotty S. A Cytokine-Independent Approach To Identify Antigen-Specific Human Germinal Center T Follicular Helper Cells and Rare Antigen-Specific CD4+ T Cells in Blood. J Immunol. 2016; 197:983–93. [PubMed: 27342848]
35. Havenar-Daughton C, Reiss SM, Carnathan DG, Wu JE, Kendric K, Torrents de la Peña A, Kasturi SP, Dan JM, Bothwell M, Sanders RW, Pulendran B, Silvestri G, Crotty S. Cytokine-Independent Detection of Antigen-Specific Germinal Center T Follicular Helper Cells in Immunized Nonhuman Primates Using a Live Cell Activation-Induced Marker Technique. J Immunol. 2016; 197:994–1002. [PubMed: 27335502]
36. Sauerbrei A, Langenhan T, Brandstadt A, Schmidt-Ott R, Krumbholz A, Girschick H, Huppertz H, Kaiser P, Liese J, Streng A, Niehues T, Peters J, Sauerbrey A, Schroten H, Tenenbaum T, Wirth S, Wutzler P. Prevalence of antibodies against influenza A and B viruses in children in Germany, 2008 to 2010. Euro Surveill Bull Eur sur les Mal Transm = Eur Commun Dis Bull. 2014; 19 available at http://www.ncbi.nlm.nih.gov/pubmed/24524235.
37. Gros A, Parkhurst MR, Tran E, Pasetto A, Robbins PF, Ilyas S, Prickett TD, Gartner JJ, Crystal JS, Roberts IM, Trebska-McGowan K, Wunderlich JR, Yang JC, Rosenberg SA. Prospective

Author Manuscript Author Manuscript Author Manuscript Author Manuscript

identification of neoantigen-specific lymphocytes in the peripheral blood of melanoma patients. Nat Med. 2016; doi: 10.1038/nm.4051

38. Weng WK, Armstrong R, Arai S, Desmarais C, Hoppe R, Kim YH. Minimal residual disease monitoring with high-throughput sequencing of T cell receptors in cutaneous T cell lymphoma. Sci Transl Med. 2013; 5:214ra171.
39. Mamedov IZ, Britanova OV, Bolotin DA, Chkalina AV, Staroverov DB, Zvyagin IV, Kotlobay AA, Turchaninova MA, Fedorenko DA, Novik AA, Sharonov GV, Lukyanov S, Chudakov DM, Lebedev YB. Quantitative tracking of T cell clones after haematopoietic stem cell transplantation. EMBO Mol Med. 2011; 3:201–7. [PubMed: 21374820]
40. Becattini S, Latorre D, Mele F, Foglierini M, De Gregorio C, Cassotta A, Fernandez B, Kelderman S, Schumacher TN, Corti D, Lanzavecchia A, Sallusto F. T cell immunity. Functional heterogeneity of human memory $CD4^+$ T cell clones primed by pathogens or vaccines. Science. 2015; 347:400–6. [PubMed: 25477212]
41. He J, Tsai LM, Leong YA, Hu X, Ma CS, Chevalier N, Sun X, Vandenberg K, Rockman S, Ding Y, Zhu L, Wei W, Wang C, Karnowski A, Belz GT, Ghali JR, Cook MC, Riminton DS, Veillette A, Schwartzberg PL, Mackay F, Brink R, Tangye SG, Vinuesa CG, Mackay CR, Li Z, Yu D. Circulating precursor CCR7(lo)PD-1(hi) $CXCR5^+$ $CD4^+$ T cells indicate Tfh cell activity and promote antibody responses upon antigen reexposure. Immunity. 2013; 39:770–81. [PubMed: 24138884]
42. Suan D, Nguyen A, Moran I, Bourne K, Hermes JRR, Arshi M, Hampton HRR, Tomura M, Miwa Y, Kelleher ADD, Kaplan W, Deenick EKK, Tangye SGG, Brink R, Chtanova T, Phan TGG. T follicular helper cells have distinct modes of migration and molecular signatures in naive and memory immune responses. Immunity. 2015; 42:704–18. [PubMed: 25840682]
43. Wallin EF, Jolly EC, Suchánek O, Bradley JA, Espéli M, Jayne DRW, Linterman MA, Smith KGC. Human T-follicular helper and T-follicular regulatory cell maintenance is independent of germinal centers. Blood. 2014; 124:2666–74. [PubMed: 25224411]
44. Linderman SL, Chambers BS, Zost SJ, Parkhouse K, Li Y, Herrmann C, Ellebedy AH, Carter DM, Andrews SF, Zheng N-Y, Huang M, Huang Y, Strauss D, Shaz BH, Hodinka RL, Reyes-Terán G, Ross TM, Wilson PC, Ahmed R, Bloom JD, Hensley SE. Potential antigenic explanation for atypical H1N1 infections among middle-aged adults during the 2013–2014 influenza season. Proc Natl Acad Sci U S A. 2014; 111:15798–803. [PubMed: 25331901]
45. Huang KYA, Rijal P, Schimanski L, Powell TJ, Lin TY, McCauley JW, Daniels RS, Townsend AR. Focused antibody response to influenza linked to antigenic drift. J Clin Invest. 2015; 125:2631–2645. [PubMed: 26011643]
46. Ekström M. Quantifying spatial patterns of landscapes. Ambio. 2003; 32:573–6. [PubMed: 15049355]
47. Gregori J, Perales C, Rodriguez-Frias F, Esteban JI, Quer J, Domingo E. Viral quasispecies complexity measures. Virology. 2016; 493:227–37. [PubMed: 27060566]
48. Zeileis, A. ineq: Measuring Inequality, Concentration, and Poverty. 2014. available at https://cran.r-project.org/package=ineq
49. Wickham, H. ggplot2: Elegant Graphics for Data Analysis. Springer-Verlag New York; New York: 2009. http://ggplot2.org
50. Warnes, G., Bolker, B., Bonebakker, L., Gentleman, R., Liaw, WHA., Lumley, T., Maechler, M., Magnusson, A., Moeller, S., Schwartz, M., Venables, B. gplots: Various R Programming Tools for Plotting Data. 2015. available at https://cran.r-project.org/package=gplots
51. Roederer M, Nozzi JL, Nason MC. SPICE: exploration and analysis of post-cytometric complex multivariate datasets. Cytometry A. 2011; 79:167–74. [PubMed: 21265010]

Author Manuscript Author Manuscript Author Manuscript Author Manuscript

One sentence summary

Repertoire studies of circulating Tfh following influenza vaccination identified a recurring oligoclonal response following successive annual vaccinations.**

Author Manuscript
Author Manuscript
Author Manuscript
Author Manuscript

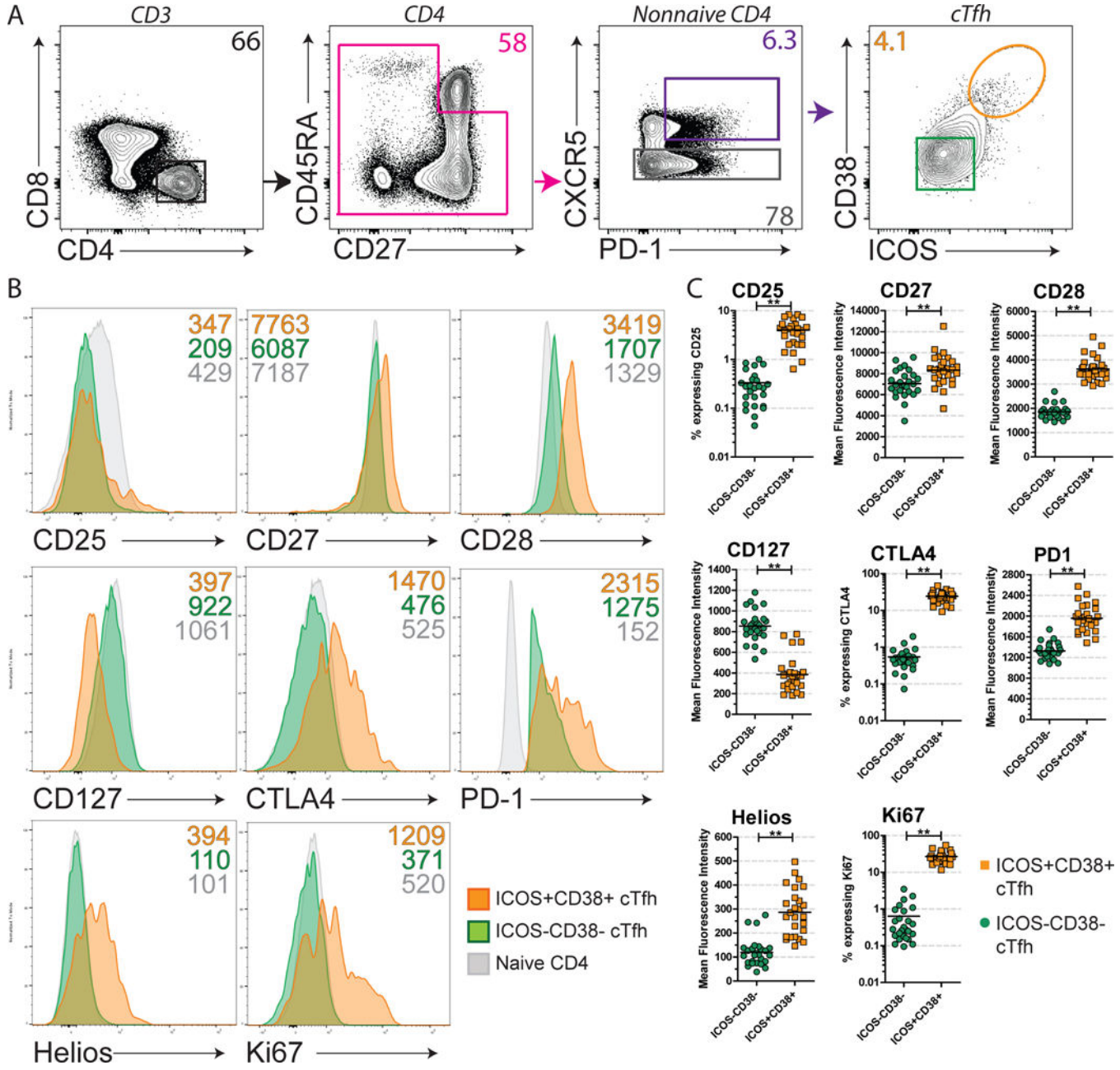

Figure 1. Circulating CXCR5+PD-1+ICOS+CD38+ cTfh express many markers of activation

A. Circulating Tfh were identified by coexpression of CXCR5 and PD-1 in CD3+CD4+ PBMC. Representative histograms (**B**) and summary plots (**C**) are shown for direct staining for cTfh for CD25, CD27, CD28, CD127, CTLA4, PD-1, Helios, and Ki67. MFI for each subset shown on the histograms. ** P<0.01 by two-tailed t-test.

Author Manuscript
Author Manuscript
Author Manuscript
Author Manuscript

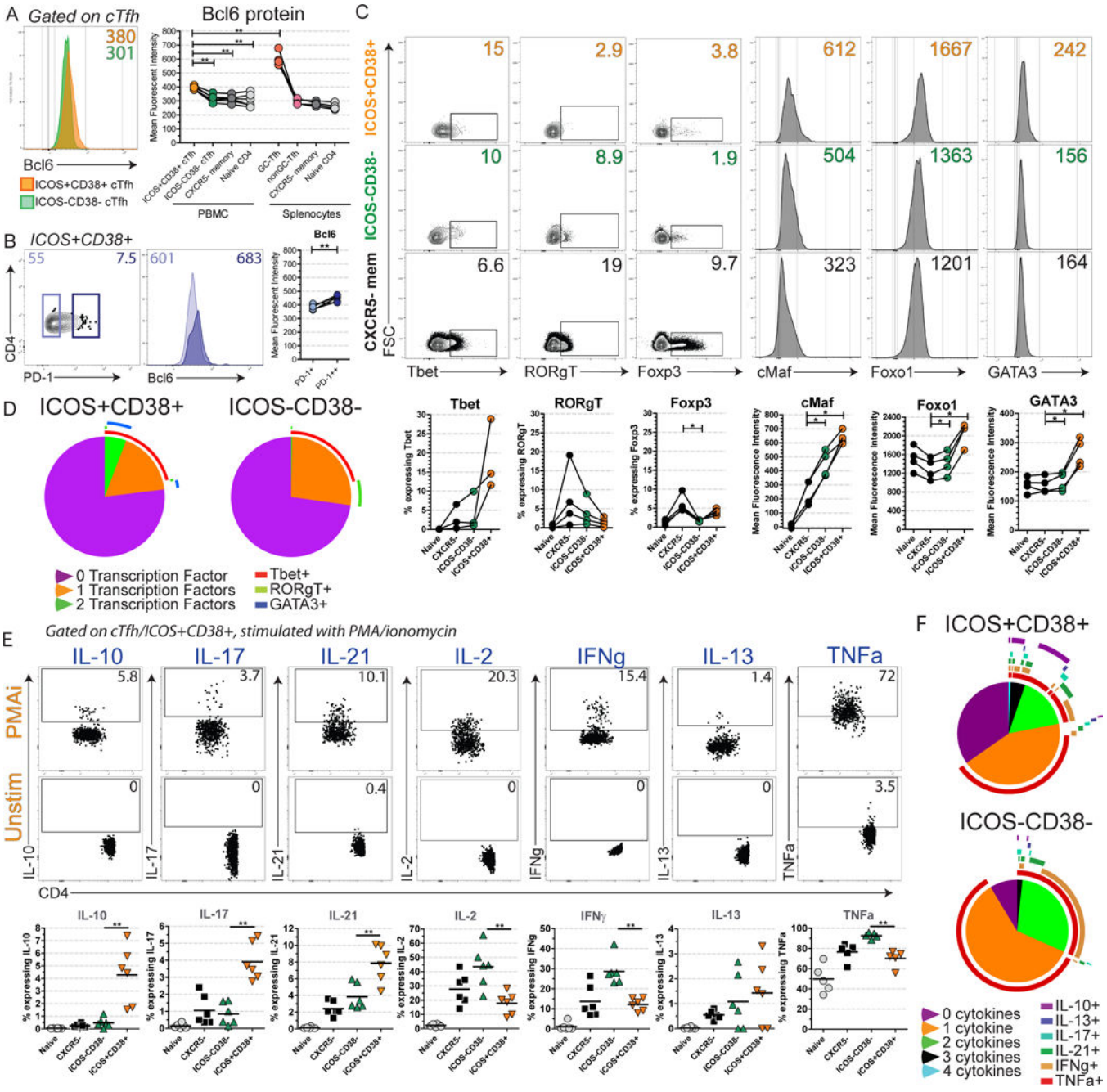

Figure 2. Activated cTfh express Bcl6 and Tbet and can produce IL-10, IL-17, and IL-21

Transcription factor and cytokine staining was performed on PBMC following isolation and permeabilization. Not all statistically significant differences are shown. *P<0.05 and **P<0.01 by repeated measures ANOVA unless otherwise indicated. **A.** Bcl6 protein expression is shown for ICOS+CD38+ and ICOS−CD38− cTfh compared to human splenic CD4 subsets. Summary plots are shown for six subjects for PBMC and four subjects for splenocytes, with lines connecting same subject. Data shown is representative of 3 independent experiments. **P<0.01 by one-way ANOVA. **B.** Bcl6 protein expression is shown for ICOS+CD38+ cTfh that were further subsetted into PD1+ and PD1++. **C.** PBMC

Author Manuscript Author Manuscript Author Manuscript Author Manuscript

were permeabilized and stained for transcription factors as shown. **D.** SPICE analysis of the transcription factors shown for ICOS+CD38+ cTfh and ICOS−CD38− cTfh. **E.** PBMC were stimulated with PMA/ionomycin for five hours at 37C with monensin added for the final four hours. Cells were fixed prior to permeabilization and intracellular staining. Summary plots and examples are shown for each cytokine. **F.** Polyfunctionality analysis was performed using the cytokines as shown.

Author Manuscript
Author Manuscript
Author Manuscript
Author Manuscript

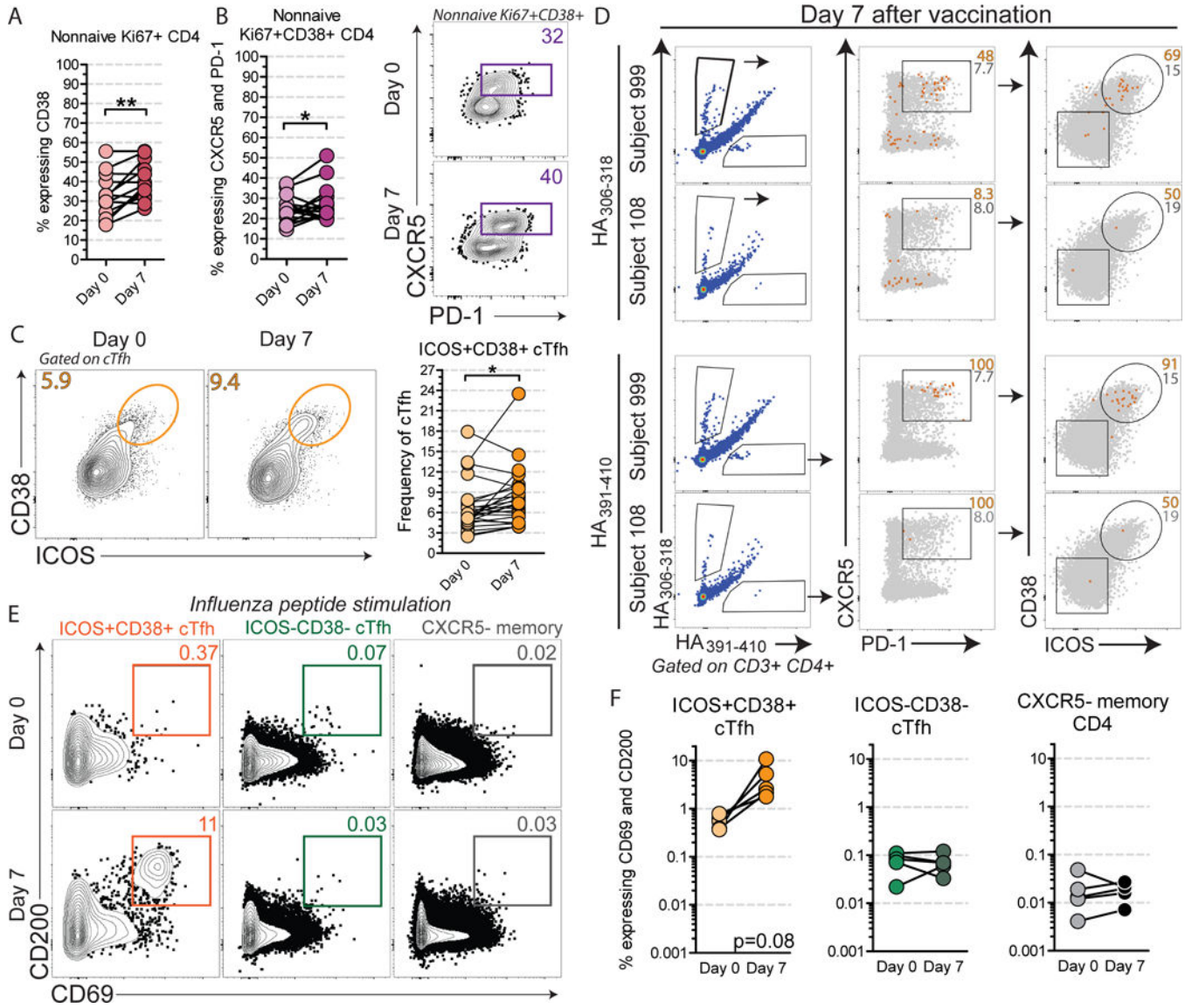

Figure 3. ICOS and CD38 identify a cTfh subset that is induced by vaccination

Adults were vaccinated with seasonal inactivated influenza vaccine and PBMC isolated at days 0 and 7. **A.** Expression of CD38 is shown in nonnaive Ki67+ CD4 at day 7 after vaccination (n=13). **P<0.01 by paired t-test. **B**. Circulating frequency of CXCR5+PD-1+ cells is shown as a proportion of the nonnaive Ki67+CD38+ CD4 population from PBMC (n=13). *P<0.05 by paired t-test. Example flow plots are shown for one subject. **C.** Expression of ICOS and CD38 for the cTfh subset at day 7 after vaccination is shown for one subject (left) and for the full cohort (right, n=28). *P=0.019 by paired t-test. **D.** MHC Class II tetramers were loaded with $HA_{306–318}$ or $HA_{398–410}$ peptides. At day 7 after vaccination, PBMC from two HLA-DRB*0401 subjects were stained for surface proteins and tetramer followed by magnetic enrichment. **E.** PBMC were stimulated for 18 hours with overlapping peptide pools for influenza proteins hemagglutinin 1, hemagglutinin 3, nucleoprotein, and matrix 1 followed by cell staining and acquisition. Example plots are shown for expression of CD69 and CD200 for different CD4 subsets. **F.** Summary plots for

CD4 subsets are shown for activation-induced markers following stimulation. P=0.08 by paired t-test for ICOS+CD38+ cTfh (left panel).

Author Manuscript Author Manuscript Author Manuscript Author Manuscript

Author Manuscript Author Manuscript Author Manuscript Author Manuscript

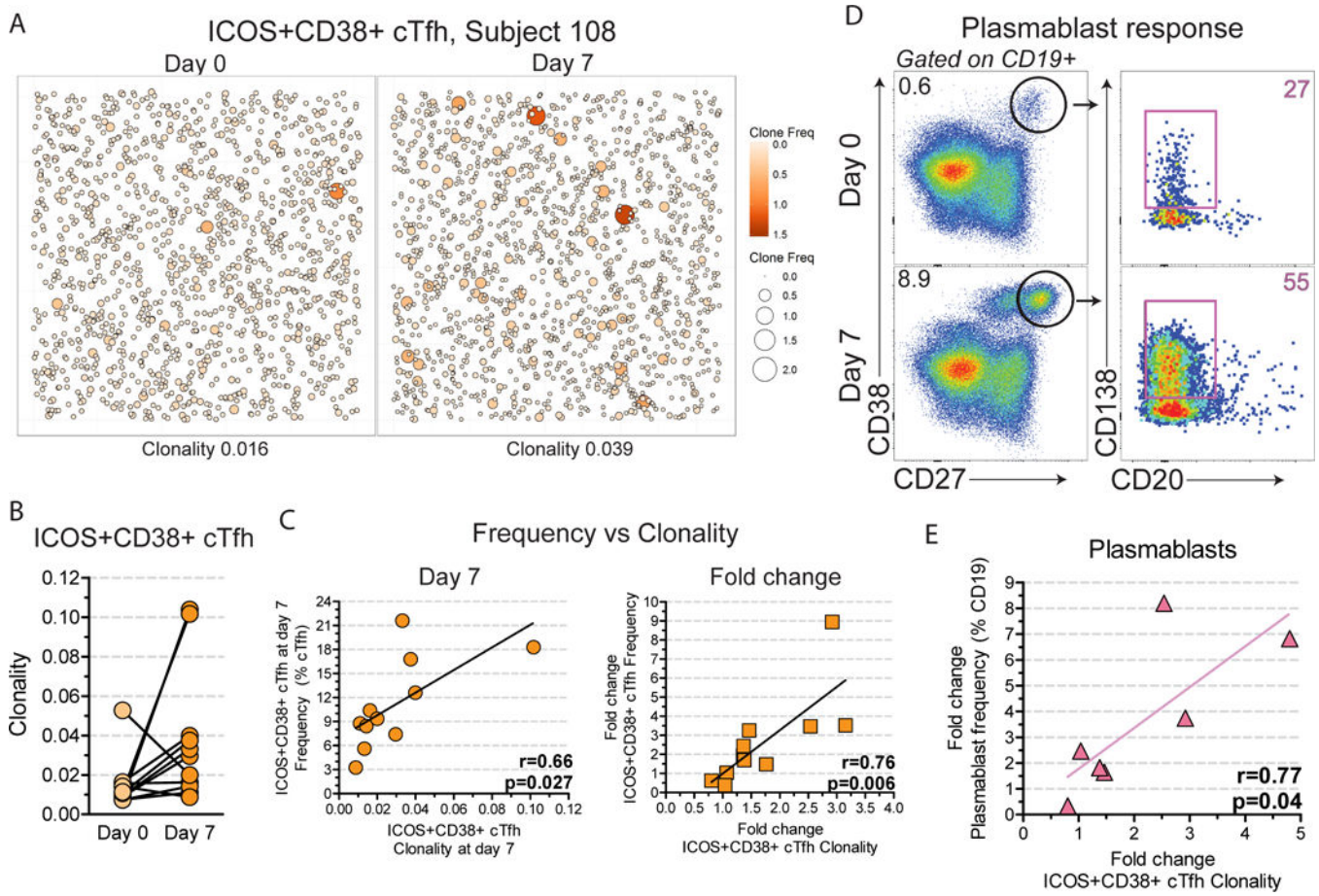

Figure 4. Increased clonality in ICOS+CD38+ cTfh correlates with plasmablast response. A All in-frame productive clonotypes from ICOS+CD38+ cTfh were plotted before and after vaccination for one subject. Each symbol indicates a unique clonotype. Clonotypes are randomly distributed across the plot, with the size and color of the symbol representing the clonal frequency. **B.** Clonality score calculations were performed for in-frame productive clonotypes at both time points for the 2015–2016 vaccination year for ICOS+CD38+ cTfh (n=11). P=0.076 by paired t-test. **C.** Day 7 clonality was correlated against the day 7 ICOS +CD38+ cTfh frequency as a percent of all cTfh (left, n=11). The fold-change in clonality was also correlated against the fold-change in ICOS+CD38+ cTfh circulating frequency (right, n=11). Pearson correlation and P value are shown. **D.** PBMC were assayed by flow cytometry at days 0 and 7 after influenza vaccination. Plasmablasts were identified as CD138+CD20− cells that were also CD19+CD27+CD38+. **E.** Pearson correlation for the fold-change between days 7 and 0 of the plasmablast frequency against the fold-change between days 7 and 0 in ICOS+CD38+ cTfh clonality score is shown (n=7).

Author Manuscript Author Manuscript Author Manuscript Author Manuscript

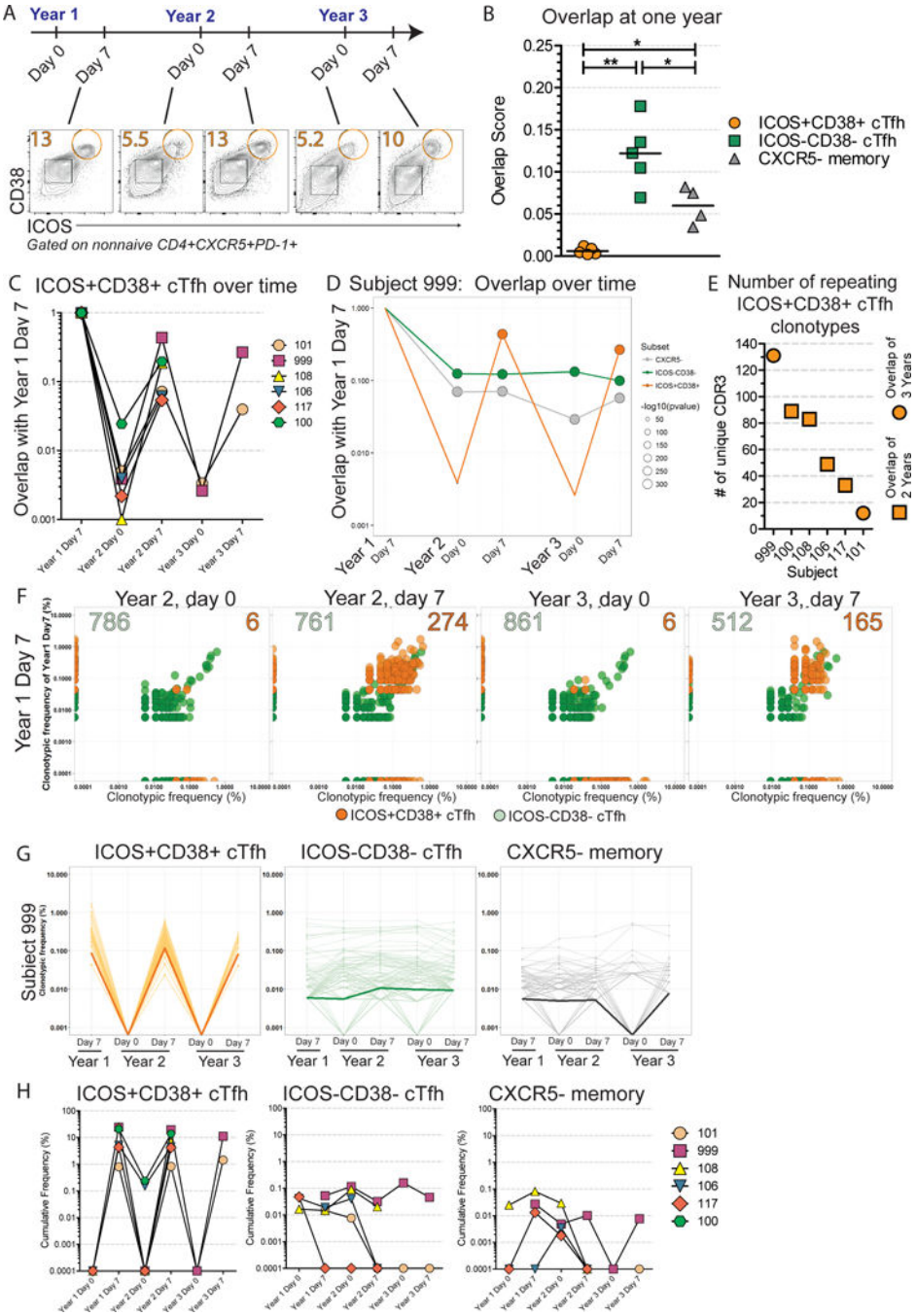

Figure 5. Repeated clonotypic response in ICOS+CD38+ cTfh identified with successive vaccinations

The subset of subjects for whom cryopreserved samples were available was assessed for year-to-year changes. **A.** Schematic to show the nomenclature used. Year 1 indicates the subject's first entry into the study, Year 2 indicates the subject's following year participation in the study. Day 0 refers to the pre-vaccination time point for the particular study year, and Day 7 refers to the one-week post-vaccination time point. Flow plots for cTfh shown for subject 999 at Year 1 Day 7, Year 2 Days 0 and 7, and Year 3 Days 0 and 7. **B.** Clonotypes

Author Manuscript Author Manuscript Author Manuscript Author Manuscript

for each subset were compared between Year 1 Day 0 and Year 2 Day 0 to determine the overlap score. *P<0.05 and **P<0.01 by one-way ANOVA with Tukey's post-hoc analysis. **C.** For each subject, Year 1 Day 7 was taken as the reference point and an overlap score was generated for each subsequent time point for ICOS+CD38+ cTfh. **D.** For each subset for subject 999, Year 1 Day 7 was taken as the reference point and overlap scores generated. ICOS+CD38+ cTfh (orange), ICOS−CD38− cTfh (green), and CXCR5− memory CD4 (grey) subsets are shown. Size of the symbol indicates the $-\log_{10}$(P value) for the Fisher's Exact test, given a theoretical repertoire of 10^7 clonotypes. **E.** Number of unique CDR3 sequences in the recurrent oligoclonal response for each subject. Squares indicate overlap across two successive vaccinations. Circles indicate overlap across three successive vaccinations. **F.** Unique clones are indicated for subject 999. The Year 1 Day 7 time point is maintained on the Y-axis in all plots, and the X-axis varies based on the time point being analyzed. Values indicate number of clonotypes overlapping between each pair of time points for ICOS+CD38+ cTfh (orange, upper right) or ICOS−CD38− cTfh (green, upper left). **G.** Clonotypic frequency for individual clonotypes that were present at Year 1 Day 7, Year 2 Day 7, and Year 3 Day 7 were plotted for each subset. Dark line used to indicate the median value at each time point for the given subset. **H.** Cumulative frequency of the recurring oligoclonal response clonotypes within the bulk TCRseq data for the different subsets over time.

Author Manuscript Author Manuscript Author Manuscript Author Manuscript

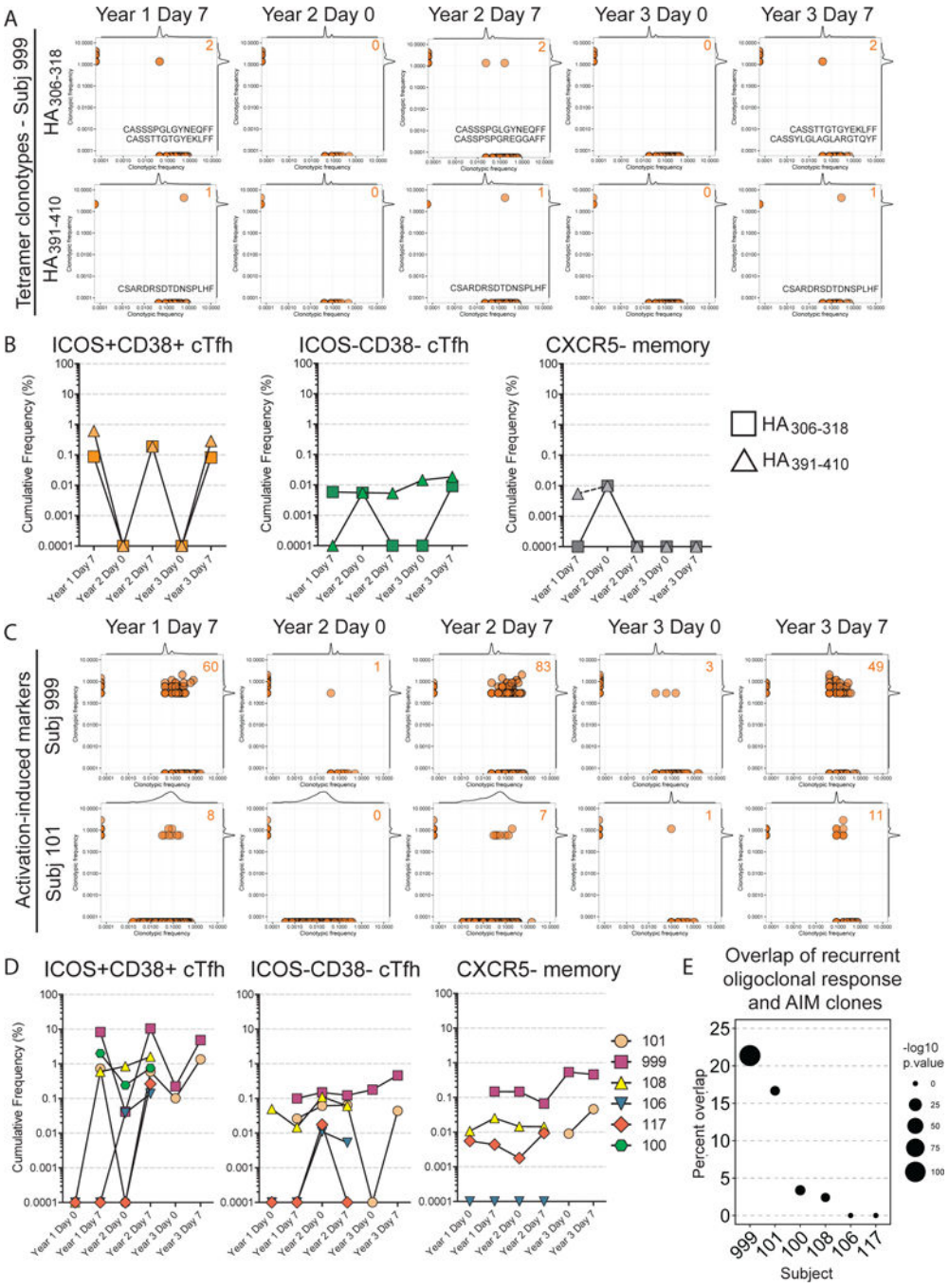

Figure 6. Tetramer and AIM clonotypes are found in the ICOS+CD38+ cTfh subset

TCRseq was performed on cells following staining for tetramer or expression of activation-induced markers following stimulation. **A.** Tetramer-positive cells were sorted six months after influenza vaccination in two HLA-DRB1*04:01 subjects. Clonotypic frequency for tetramer (x-axis) is plotted against for the bulk ICOS+CD38+ cTfh subset (y-axis) at various time points. Marginals on the outer edges show the single-axis histogram for individual axes. Number of overlapping clones (upper right) and CDR3 sequences for the overlapping clones (bottom right) are indicated. **B.** Cumulative frequency of tetramer clones within the bulk

Author Manuscript Author Manuscript Author Manuscript Author Manuscript

TCRseq data for different subsets is shown. Squares indicate $HA_{306–318}$ tetramer clonotypes whereas triangles indicate $HA_{398–410}$ tetramer clonotypes. **C.** PBMC were stimulated for 18 hours with overlapping peptide pools for influenza proteins and ICOS+CD38+ cTfh that expressed CD69 and CD200 were sorted for TCRseq. Clonotypic frequency for AIM clonotypes is plotted for the bulk ICOS+CD38+ cTfh subset at various time points. Marginals on the outer edges show the single-axis histogram for individual axes. Number of overlapping clones is given in the plot. **D.** Cumulative frequency of AIM clones within the bulk TCRseq data for different subsets is shown. Connected symbols show repeated observations for the same subject over time. **E.** Percent overlap in unique CDR3 sequences is shown between the recurring oligoclonal response and the AIM clonotypes for each subject. Size of the symbol indicates $-\log_{10}$(P value) as assessed by Fisher's Exact test, assuming 10^7 possible clonotypes.

Author Manuscript Author Manuscript Author Manuscript Author Manuscript

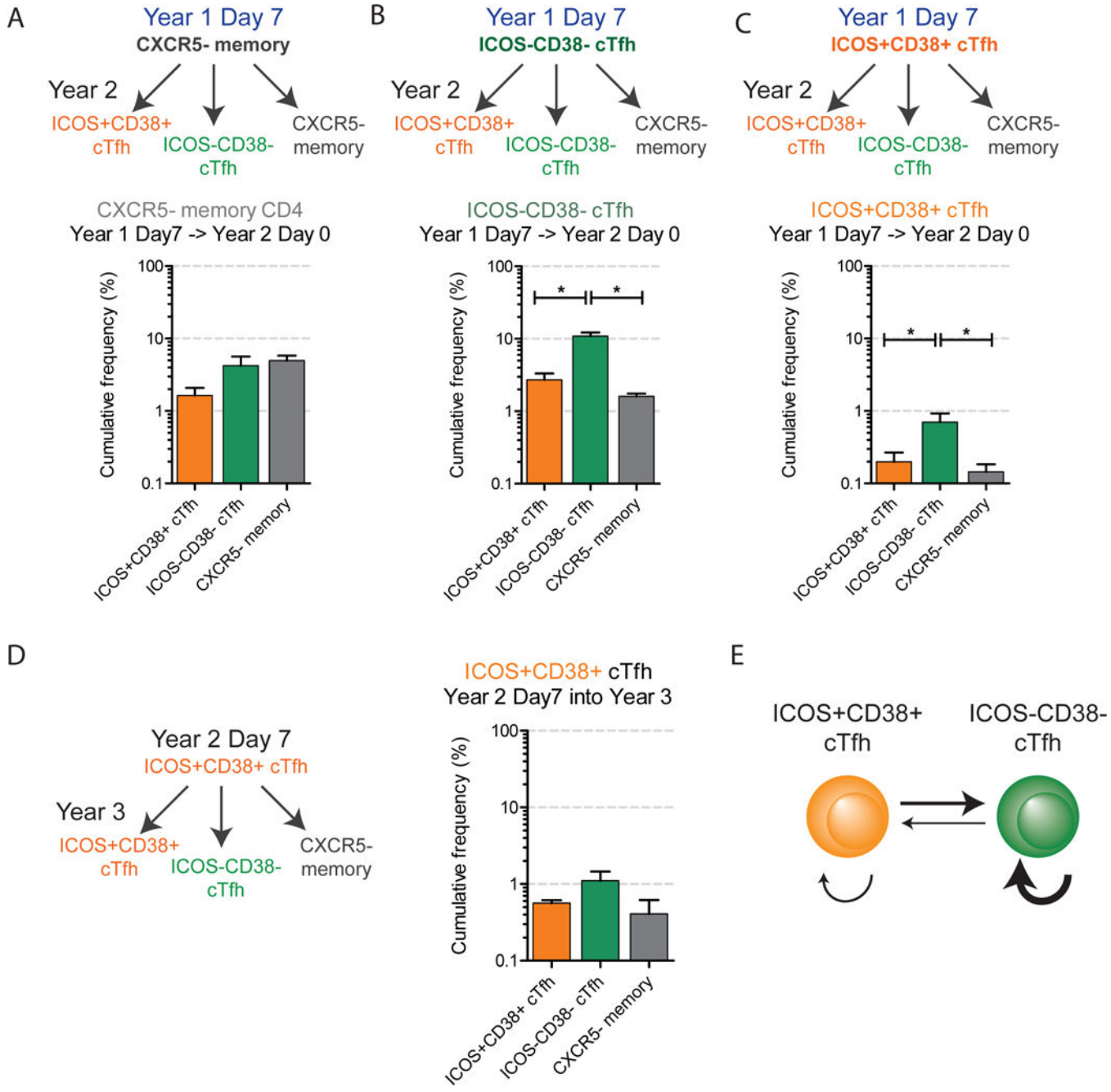

Figure 7. ICOS+CD38+ cTfh clonotypes are later found in other subsets

Orange indicates the ICOS+CD38+ cTfh subset, Green indicates the ICOS−CD38− cTfh subset, and Grey indicates the CXCR5− memory subset. **A–C.** Clonotypes that were present in Year 1 Day 7 for the indicated subset were then evaluated in all three subsets in Year 2 for Days 0. *P<0.05 by repeated-measures ANOVA with Tukey's post-test. **D.** Clonotypes that were present in Year 2 Day 7 for subjects 101 and 999 were assessed in all three subsets for Year 3 Day 0. Cumulative clonotypic frequency is shown. **E.** Proposed directionality of intersubset changes based on panels **A–C**.